

Reintroduction of ionic structure in the self-consistent jellium model for metal clusters: Pseudopotential perturbation theory

W.-D. Schöne and W. Ekardt

Fritz-Haber-Institut der Max-Planck-Gesellschaft, Faradayweg 4-6, 14195 Berlin, Germany

J. M. Pacheco

Departamento de Física da Universidade, 3000 Coimbra, Portugal

(Received 2 May 1994)

The structureless self-consistent jellium model for simple metal clusters is corrected by reintroducing the ionic structure via second-order pseudopotential perturbation theory. It is found that this formulation is enough to bring this approximate treatment into a quantitative agreement with fully fledged *ab initio* Car-Parrinello structure optimization. Furthermore, the ionic perturbation leads to a substantial improvement in the description of the optical response.

I. INTRODUCTION

It is well known for bulk forms of simple metals that the self-consistent jellium model is able to describe, at least qualitatively, the excitation of plasmons,¹ constituting a first step towards a realistic description of the dynamical behavior of electrons. In this spirit, the self-consistent jellium model for metal clusters has been proposed by one of us.² It became, since then, the most used model for all kinds of metallic atomic clusters, and has boosted many extensions, modifications, and approximations. To this popularity the success of the jellium model in describing many properties of clusters is not alien, including some fine features of their optical response, with respect to which this model remains to be superseded (for a review cf., e.g., Ref. 3).

On the other hand, it is also well established⁴ for bulk metals that, whenever one wants to have a quantitative prediction of cohesive energies, work function, or plasmon dispersion curves, the pure jellium calculations have to be complemented by a reintroduction of the ionic structure. For the simple alkaline metals, the associated pseudopotentials are very weak, and one may reintroduce the ionic structure using perturbation theory. Pseudopotential perturbation theory has proved very successful in connection with lattice relaxation at metal surfaces.¹¹ It is, therefore, natural to study the effects of the ionic structure in metal clusters along similar lines. This project is started in the present work, in which a detailed study of ionic structure effects on the electronic properties of metal clusters is carried out, via the reintroduction of the ionic structure in the jellium model by means of second-order pseudopotential perturbation theory. In this work, we shall investigate structural ground-state properties, as well as the optical response of neutral sodium microclusters. In a first step, we shall concentrate on closed-shell sodium clusters, computing their optical response in a spherical approximation. In a second step, we shall investigate open-shell clusters, and compute their optical response making use of pseudopotential per-

turbed response. Finally, we apply the perturbed response formulation to the closed-shell systems, demonstrating the validity of the spherical approximation for these type of clusters.

It will be found that the main role (for magic clusters) played by the ionic structure is to fix the volume of delocalization for the valence electrons. In fact, from the results of the present paper, one can infer that the correct volume of delocalization, together with the global shape of the cluster are the basic ingredients characterizing its optical response. For the small clusters treated here, surface quantization determines the main features of the optical spectra, whereas genuine band-structure effects such as bulk quantization are less pronounced. In a sense, this was to be expected, due to the excellent performance of both the spherical^{2,5} and spheroidal⁶ jellium models which, even at the level of one-electron orbital energies, lead to very good results as compared to *ab initio* calculations, as well as to level splittings in excellent agreement with experimental findings.⁷ Finally, the results of the present paper corroborate the picture of the jellium model as an excellent starting point for metal cluster calculations.

Among the simple metals, sodium is perhaps the one which is best described by local pseudopotentials. Many local pseudopotentials for sodium exist in the literature, and among these we shall adopt two, the parameters of which have been obtained using radically different phenomenological methods. This will put in evidence the dependence of the results of the specific parametrizations used, as well as on the methods employed in such parametrizations. *Ab initio* pseudopotentials, on the other hand, are typically nonlocal. While these nonlocal effects are small for sodium, the method developed here is independent of the particular form or local character of the pseudopotential. In particular (see below), the present formulation provides a physical and simple way to introduce the ionic structure into the structureless jellium model, and it constitutes a natural way to introduce non-local or semilocal pseudopotential effects. This is to be

contrasted with a recent study of the static and dynamic properties of lithium clusters,⁸ in which the contribution of the jellium background was replaced by a spherically symmetric, nonlocal external field. Since no geometrical effects due to the ionic structure are incorporated, resulting in a structureless external potential, the model constitutes a nonlocal version of the well-known pseudojellium model of Utreras-Diaz and Shore,⁹ or of the stabilized jellium model of Perdew, Tran, and Smith.¹⁰

In this paper, we make use of the following pseudopotentials:

(1) The Heine-Abarenkov pseudopotential (HA-PSP), with parameters chosen to fit relevant bulk properties,¹¹ such as bulk compressibility and lattice parameter and used to determine vacancy formation energies;

(2) The empty-core Ashcroft pseudopotential (A-PSP), with its single parameter fixed in order to fit the single-particle energy of the valence electron in the alkaline atom and used in the study of clusters within the so-called spherical average pseudopotential (SAPS) model.¹² These pseudopotentials will mimic the constituent ions of the cluster and their interaction with the valence electrons.

The reintroduction of the ionic structure on the jellium model brings along several effects, which can be viewed as acting to change different quantities entering the well-known surface-plasmon formula for a spherical particle:

$$\omega_s = \frac{4\pi n_0 e^2}{m_0} / \sqrt{3} . \quad (1)$$

Specifically, one may expect (1) changes in the effective density n_0 of the delocalized electrons, (by replacing the jellium background radius R with a better definition); (2) changes in the coupling constant e^2 for collective motion, for instance, because of screening as a result of core-polarizability $\epsilon_c(e^2 \rightarrow e^2/\epsilon_c)$; and (3) changes in the effective mass m_0 (due to many-body-renormalization effects and because of nonlocal pseudopotentials⁸).

Of all these effects, only item 1 will be covered in this paper, whereas items 2 and 3 are deferred to a future study.

This paper is organized as follows: In Sec. II the theoretical model we use is presented. Section III is devoted to the presentation and discussion of the results obtained, both for the ground state (Sec. III A) and optical absorption (Sec. III B). Finally, the main conclusions are included in Sec. IV.

II. THEORY

A. Ground state

The underlying assumption for the feasibility of the concept of a sharp-edge jellium model plus pseudopotential perturbation theory is that it makes sense to treat the loosely bound valence electrons and the tightly bound core electrons in a completely different way: At any size, the latter are considered to be frozen in their core orbitals whereas the former are responsible for binding the atoms into a cluster. The nature of this binding is metallic for

all sizes, so that correlation energy is gained by the delocalized electrons. In this way, the valence electrons interact with the ions via weak pseudopotentials. The resulting electron-ion interaction can then be written in the form,

$$v_{\text{ex}}(\mathbf{r}, \mathbf{R}) = \sum_{i=1}^N v_{\text{ps}}(\mathbf{r} - \mathbf{R}_i), \quad \mathbf{R} = \{\mathbf{R}_i\} . \quad (2)$$

In this equation, \mathbf{R} is to be determined by minimizing the total energy of the system. This has already been done by Röthlisberger and Andreoni,¹³ within the Car-Parinello method. Because our main intention is the study of the effects of the ionic structure on the optical properties of metallic clusters, we do *not* repeat this geometry optimization, but instead rely on the results of Ref. 13, which we shall adopt as a starting point of our own calculations.

With respect to any chosen center of the cluster, the sum of the pseudopotentials can be expanded as follows:

$$\begin{aligned} v_{\text{ex}}(\mathbf{r}, \mathbf{R}) &= v(r, \mathbf{R}) + v_{2,\text{ex}}(\mathbf{r}, \mathbf{R}) \\ &= v_0(r, \mathbf{R}) Y_{0,0}(\hat{\mathbf{r}}) \\ &\quad + \sum_{l=1}^{\infty} \sum_{m=-l}^l v_{l,m}(r, \mathbf{R}) Y_{l,m}(\hat{\mathbf{r}}) . \end{aligned} \quad (3)$$

The first term is just the monopole, spherical part of the total ionic contribution, which is taken into account exactly by solving the set of Kohn-Sham equations for the N valence electrons moving self-consistently in this external potential. When only this monopole part of the ionic contribution is used in geometry optimization and optical response calculations, one obtains the SAPS model developed by Iñiguez, Lopez, and Alonso.¹² This, as will be shown below, does not contain enough information of the cluster-ionic structure, which makes ground-state geometry optimization converge to shapes corresponding to excited configurations of the clusters and also to volumes of delocalization for the valence electrons which are markedly different from the ones obtained with the present formulation.

In our formulation, we include the second part of the pseudopotential sum in Eq. (3) perturbatively up to second order, which leads to the following contribution to the total energy:

$$\Delta E_{\text{ps}} = \Delta E_{\text{ps}}^{(1)} + \Delta E_{\text{ps}}^{(2)} , \quad (4)$$

with

$$\Delta E_{\text{ps}}^{(1)} = \int d\mathbf{r} n_{\text{SAPS}}(\mathbf{r}, \mathbf{R}) v_{2,\text{ex}}(\mathbf{r}, \mathbf{R}) , \quad (5)$$

and

$$\begin{aligned} \Delta E_{\text{ps}}^{(2)} &= \frac{1}{2} \int d\mathbf{r} \delta n_2(\mathbf{r}, \mathbf{R}) v_{2,\text{ex}}(\mathbf{r}, \mathbf{R}) \\ &= \frac{1}{2} \int d\mathbf{r} d\mathbf{r}' v_{2,\text{ex}}(\mathbf{r}, \mathbf{R}) \\ &\quad \times \chi_{\text{SAPS}}(\mathbf{r}, \mathbf{r}', \mathbf{R}) v_{2,\text{ex}}(\mathbf{r}', \mathbf{R}) . \end{aligned} \quad (6)$$

$n_{\text{SAPS}}(\mathbf{r}, \mathbf{R})$ is the self-consistent ground-state density and $\delta n_2(\mathbf{r}, \mathbf{R})$ the induced screened density change caused by the external potential $v_{2,\text{ex}}(\mathbf{r}, \mathbf{R})$. Clearly, the first-order

part vanishes identically, due to the orthogonality of the spherical harmonics.

In order to calculate the second-order correction, we have to calculate the static electronic susceptibility at the SAPS level,¹² that is, using the one-electron states of the spherical potential $v(r, \mathbf{R})$, which can be readily carried out in a numerically exact way via Green's functions methods^{5,14}. Once the ionic structure which minimizes the total energy (including the perturbation correction) has been determined, we can compute the frequency-dependent susceptibility at the SAPS level, in order to study the optical response of the metal clusters. Due to this spherical symmetry of the SAPS model, we concentrate on spherical-like closed-shell systems such as Na₈ and Na₂₀.

All calculations have been carried out using the same methods employed in the standard jellium model for metal clusters,^{2,14} namely, density-functional theory (DFT) in the local-density approximation. The response calculations (also the computation of the static susceptibilities) have been carried out at the level of time-dependent local-density approximation (TDLDA). Details of these methods as applied to spherical many-electron systems can be found, for instance, in Ref. 14.

B. Optical response

At the TDLDA level, any calculation starts with the calculation of the independent-particle susceptibility

$$\begin{aligned} \chi_0(\mathbf{r}, \mathbf{r}_1; \omega) = & 2 \sum_i \psi_{n_i, l_i, m_i}^*(\mathbf{r}) \psi_{n_i, l_i, m_i}(\mathbf{r}_1) \\ & \times G^R(\mathbf{r}, \mathbf{r}_1; \epsilon_{n_i, l_i, m_i} + \hbar\omega) \\ & + 2 \sum_i \psi_{n_i, l_i, m_i}(\mathbf{r}) \psi_{n_i, l_i, m_i}^*(\mathbf{r}_1) \\ & \times G^{R*}(\mathbf{r}, \mathbf{r}_1; \epsilon_{n_i, l_i, m_i} - \hbar\omega). \end{aligned} \quad (7)$$

If the SAPS is used as the cluster model [first part of the potential Eq. (3)], the wave functions of the occupied states and the retarded Green's functions of this Kohn-Sham operator are inserted; because the problem is still spherically symmetric, all the calculations are nearly identical with the spherical jellium model calculations described in detail in Ref. 14. The only effect of the ions consists in a change of volume of delocalization of the valence electrons. That means the radius of the standard jellium model is replaced with a "better" definition of the volume. As we shall see later the difference is not very pronounced, in this way justifying the original assumption about the radius of the standard jellium model.

The SAPS model is approximately sufficient for magic clusters, because they are nearly spherical. In contrast it is clearly insufficient for the open-shell clusters, because they are definitely nonspherical. In these cases, we need to include the effects of the second part of the external potential in Eq. (3), both in the ground state and on the excitation process. This is done in the following way.

First, we perform a perturbation-theoretical calculation

for degenerate states of the SAPS eigenspaces in exactly the same way as it is described in the textbook by Bransden and Joachain.¹⁵ As a result, the irreducible representations of the rotation group are replaced with those of the pertaining point group. Because all the calculations are described very detailed in Ref. 15, we do not reproduce any further formulas.

Next, we determine the perturbed Green's operator G , which is quite generally a solution of

$$[\epsilon_{n, l, m} + \hbar\omega + \nabla^2 - v(\mathbf{r})] G^R(\mathbf{r}, \mathbf{r}_1; \epsilon_{n, l, m} + \hbar\omega) = \delta(\mathbf{r} - \mathbf{r}_1). \quad (8)$$

In the spirit of perturbation theory we write

$$\epsilon_{n, l, m} + \hbar\omega = \epsilon_{n, l} + \hbar\omega + \lambda \epsilon_{n, l, m}^{(1)} + \dots \quad (9)$$

$$v(\mathbf{r}) = v_{\text{eff}}(\mathbf{r}) + \lambda v_{2, \text{eff}}(\mathbf{r}) + \dots \quad (10)$$

$$\begin{aligned} G^R(\mathbf{r}, \mathbf{r}_1; \epsilon_{n, l, m} + \hbar\omega) = & G^{R(0)}(\mathbf{r}, \mathbf{r}_1; \epsilon_{n, l, m} + \hbar\omega) \\ & + \lambda G^{R(1)}(\mathbf{r}, \mathbf{r}_1; \epsilon_{n, l, m} + \hbar\omega) + \dots \end{aligned} \quad (11)$$

v_{eff} and $v_{2, \text{eff}}$ are the screened potentials corresponding to the densities $n_{\text{SAPS}}(\mathbf{r}, \mathbf{R})$ and $\delta n_2(\mathbf{r}, \mathbf{R})$ of the last paragraph. With all these equations it is an easy task to show that

$$\begin{aligned} G^{R(1)}(\mathbf{r}, \mathbf{r}_1; \epsilon_{n, l, m} + \hbar\omega) = & \int d\mathbf{r}' G^{R(0)}(\mathbf{r}, \mathbf{r}'; \epsilon_{n, l} + \hbar\omega) \\ & \times [v_{2, \text{eff}}(\mathbf{r}') - \epsilon_{n, l, m}^{(1)}] \\ & \times G^{R(0)}(\mathbf{r}', \mathbf{r}_1; \epsilon_{n, l} + \hbar\omega). \end{aligned} \quad (12)$$

If we now insert all these expansions in the general Eq. (7) for the susceptibility, the corresponding expression for this quantity becomes

$$\chi_0(\mathbf{r}, \mathbf{r}_1; \omega) = \chi_0^{(0)}(\mathbf{r}, \mathbf{r}_1; \omega) + \chi_0^{(1)}(\mathbf{r}, \mathbf{r}_1; \omega) + \dots \quad (13)$$

Because of the nonspherical nature of the problem the TDLDA integral equation can no longer be transformed to a one-dimensional one. For this reason, it is not recommendable to solve for the dressed susceptibility, but instead to determine the induced charge density directly [by iteration, where the iteration is started with Eq. (15)]

$$\delta n_1(\mathbf{r}; \omega) = \int d\mathbf{r}_1 \chi_0(\mathbf{r}, \mathbf{r}_1; \omega) v_{1, \text{eff}}(\mathbf{r}_1; \omega), \quad (14)$$

with the independent particle induced density given by (sometimes called free response)

$$\delta n_{0,1}(\mathbf{r}, \omega) = \int d\mathbf{r}_1 \chi_0(\mathbf{r}, \mathbf{r}_1; \omega) v_{1, \text{ext}}(\mathbf{r}_1; \omega) \quad (15)$$

(for details see Ref. 14). Of course the total perturbing potential $v_{1, \text{eff}}(\mathbf{r}; \omega)$ in Eq. (14) consists of the external photon field $v_{1, \text{ext}}(\mathbf{r}; \omega)$ and the total induced one as discussed in length in (Ref. 14). Once the self-consistent solution of Eq. (14) is obtained the cross section is given by the standard formulas

$$\sigma(\omega) = \frac{4\pi\omega}{c} \text{Im}(\alpha(\omega)), \quad (16)$$

where $\alpha(\omega)$ is

$$\alpha(\omega) = -e^2 \int d\mathbf{r} \delta n_1(\mathbf{r}, \omega) v_{1,\text{ext}}(\mathbf{r}, \omega). \quad (17)$$

Of course, because of the low symmetry of the open-shell cluster the result of this procedure depends on the direction of the external field. Assuming statistical orientation of the clusters in the beam, the actual cross section is obtained by the statistical average of three different directions, say x , y , and z . The results are presented for Na_6 and Na_{10} in the next section.

III. RESULTS AND DISCUSSION

A. Ground state

1. Closed-shell systems

Our calculations take, as a starting point, the global minimum-energy structure and low-lying isomers found in Ref. 13, in which geometry optimization was carried out in a fully relaxed way, using the Car-Parrinello method. Our method can, at best, reproduce the structures obtained in Ref. 13 (being, however, several orders of magnitude faster).

We put emphasis on two basis features of the ionic structure: its symmetry and, for each symmetry, the bond lengths, which define the cluster volume. We do not expect the underlying symmetry of the ionic structure to depend sensitively on the specific parametrization of the pseudopotential.¹⁶ On the other hand, we expect the pseudopotential parameters to play a decisive role in determining the volume of delocalization for the valence electrons. In keeping with this discussion, we calculate the total energy for some selected geometries found in Ref. 13, scaling the coordinates \mathbf{R} so as to keep the symmetry of the ionic arrangement, but change the magnitude of the bond lengths, in order to see for which value of this scaling parameter the minimum is obtained. As will be shown below, this restricted parameter space is enough for our purposes. Specifically, we considered three structures for Na_8 , displayed in Fig. 1, with sym-

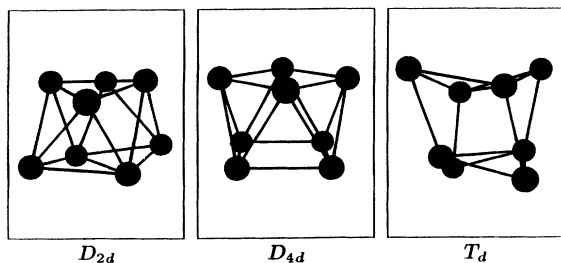


FIG. 1. The three different geometries obtained in Ref. 13 for Na_8 , corresponding to the ground state and two lowest isomers (energy is increasing from left to right), and used as our starting geometries which we minimize as a function of a dimensionless scaling parameter $0.90 \leq \eta \leq 1.10$ which simply uniformly and simultaneously changes the radial distances of all the atoms with respect to the center of mass of the cluster. The structure on the left displays D_{2d} symmetry, the one in the middle D_{4d} symmetry, and the one on the right T_d symmetry (see main text for details).

metries (in ascending order of total energy) D_{2d} , D_{4d} , and T_d . Within DFT there is a consensus that indeed the D_{2d} structure corresponds to the ground state, although different pseudopotentials lead to different bond lengths (compare Refs. 13 and 17). On the other hand, the T_d symmetry considered here, and taken from Ref. 13, corresponds to the ground-state ionic configuration resulting from a self-consistent all-electron Hartree-Fock total-energy minimization.¹⁸ It is noteworthy that within Hartree-Fock, not only the geometry found is different, but also the bond lengths are larger. In fact, the average bond length obtained in the framework of Ref. 18 for Na_8 is larger than what is known from the bulk (cf., e.g., Fig. 15 of Ref. 13), in contradiction with the well-established observation of a (small) lattice contraction as the particle size is reduced.¹⁹ As for Na_{20} , two close lying isomers were found in Ref. 13. They are displayed in Fig. 2, and will be taken as our starting geometries.

For both clusters, we varied the scaling parameter from 0.90 to 1.10, corresponding to volume changes up to 30%. We computed the total energy for each scaling parameter both at the SAPS level ($E^{(0)}$ in tables) and including second-order corrections ($E^{(2)}$ in tables). We carried out the minimizations making use of the two pseudopotentials already mentioned, namely, the HA-PSP (Ref. 11) (subscript HA in tables) and the A-PSP (Ref. 12) (subscript A in tables). The results are displayed in Tables I and II, for Na_8 and Na_{20} , respectively, where we show the scaling parameter corresponding, in each case, to the minimum energy, as well as the energy difference (in eV), taking as a reference the minimum value obtained among all energies. This, of course, was carried out separately for each pseudopotential, which means that there are two reference states for each cluster.

Several important features emerge from Tables I and II. First of all, one can see that when the energy which is minimized includes the second-order correction ($E^{(2)}$) we obtain, for the lowest configuration, the same symmetry as obtained in the fully relaxed minimization.¹³ This result is independent of the pseudopotential, the main effect of which is to fix the equilibrium bond lengths, reflected in the tabulated values for the scaling parameter at minimum. On the other hand, from Table I it becomes

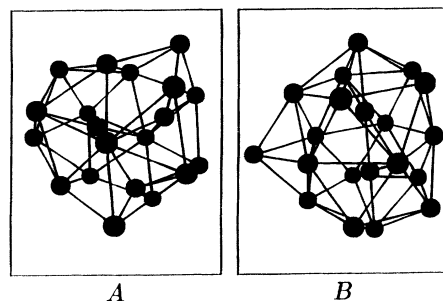


FIG. 2. The two lowest structures, A and B, obtained in Ref. 13 for Na_{20} , corresponding to the ground state (A) and to the first isomer (B), and used as our starting geometries which we minimize as a function of a dimensionless scaling parameter η (see caption to Fig. 1).

TABLE I. Results for the static properties of Na_8 , making use of two different pseudopotentials: The HA-PSP, denoted with subscript HA, and the A-PSP, denoted with subscript A. For each of the three geometries selected (cf. Fig. 1), two sets of values are given, associated to the result of a total-energy minimization as a function of the scaling parameter. The value of the scaling parameter at minimum is given in parentheses (for the meaning of this number see the main text), whereas the value of the total-energy constitutes the other result tabulated. $E^{(0)}$ corresponds to minimization using the SAPS expression for the total energy, whereas in $E^{(2)}$ the contribution from second-order pseudopotential perturbation theory is included. The values quoted for the energies are referred to the state which, for a given pseudopotential, corresponds to the absolute minimum, namely, $E^{(2)}$ for the D_{2d} symmetry. All energies are given in electron volts.

Na_8	D_{2d}	D_{4d}	T_d
$E_{\text{HA}}^{(0)}$	1.552(1.06)	1.342(1.06)	2.093(1.04)
$E_{\text{HA}}^{(2)}$	0.000(1.02)	0.108(1.02)	0.160(1.00)
$E_A^{(0)}$	2.568(1.02)	2.322(1.00)	3.118(1.00)
$E_A^{(2)}$	0.000(0.96)	0.181(0.94)	0.186(0.94)

clear the SAPS model is too crude to be able to provide the correct ground state, irrespective of the pseudopotential parametrization, since, at this level of approximation, the minimum-energy configuration corresponds to isomeric states in the fully relaxed minimization of Ref. 13. Furthermore, the results of Tables I and II seem to indicate that the HA-PSP parametrization¹¹ is superior for the study of sodium clusters. Indeed, it is worth mentioning that with this pseudopotential, our results lead to bond lengths for both Na_8 and Na_{20} which are systematically 2% larger than the ones of Ref. 13. Since the results of Ref. 13 lead to bond lengths for the dimer and bulk limits which are 2% smaller, this may indicate that we are getting the right bond lengths. Note, in passing, that the pseudopotential used in Ref. 13 leads, e.g., to a bond length in both the dimer and the bulk which is 2% below the experimental value, a result which superseeds most of the available quantum chemical calculations.²⁰

In Fig. 3 is shown, with a full line, the self-consistent densities, potentials, and eigenvalues, solutions of the Kohn-Sham equations using as an external field, the monopole part of the ionic pseudopotential, $v(r, \mathbf{R})$ [cf. Eq. (3)]. With dashed lines, we show the corresponding quantities calculated in the jellium model, taken from Ref. 14, and which are, on the whole, very similar to the pseudopotential results. In turn, this similarity corro-

TABLE II. Results for the static properties of Na_{20} , using the same notation as in Table I. The A and B structures for Na_{20} correspond to the ones shown in Fig. 2.

Na_{20}	A	B
$E_{\text{HA}}^{(0)}$	5.223(1.06)	5.191(1.08)
$E_{\text{HA}}^{(2)}$	0.000(1.02)	0.197(1.02)
$E_A^{(0)}$	7.700(1.02)	7.646(1.02)
$E_A^{(2)}$	0.000(0.94)	0.269(0.94)

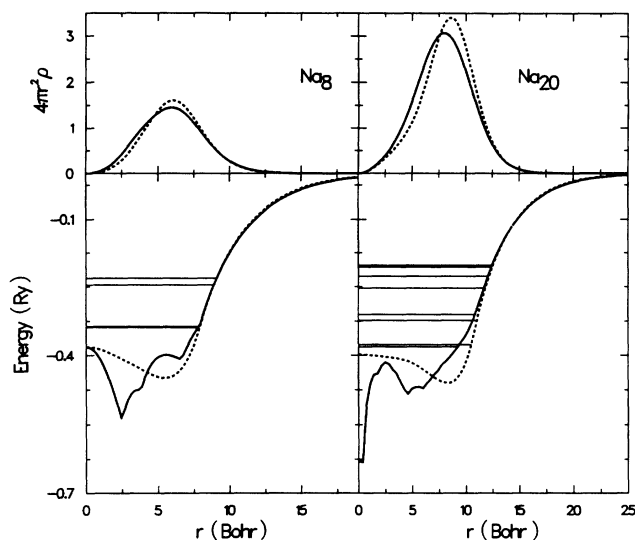


FIG. 3. Self-consistent densities (upper part), potentials and eigenvalues (lower part), solutions of the Kohn-Sham equations with two different ionic backgrounds: The spherical component of the HA-PSP (full lines), and the spherical jellium background model (dashed lines).

borates the picture of the jellium model as constituting an excellent starting point. The spikes present in the self-consistent potential associated with the pseudopotential results are well known, and characteristic of this type of calculations.¹² The self-consistent potential is, however, everywhere finite and continuous, posing no problems in the determination of the eigenvalues and the single-particle Green's functions.

Finally, there is another effect in second-order pseudopotential perturbation theory which does not emerge directly from Tables I and II. Indeed, we show in Fig. 4 the total energy of Na_8 , for the D_{2d} structure, as a function of scaling parameter, making use of the HA-PSP.

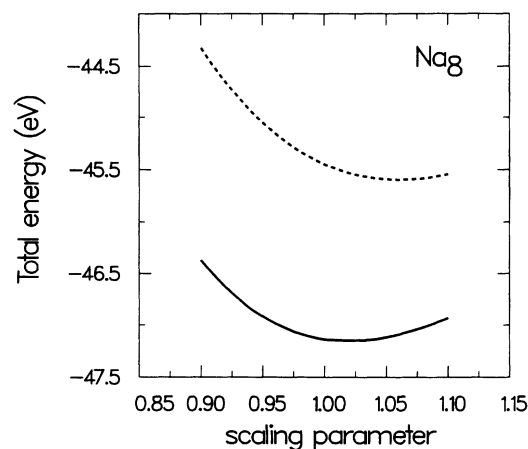


FIG. 4. Total energy of Na_8 as a function of the scaling parameter η (see main text for details), calculated as the SAPS level (dashed line) and including second-order pseudopotential perturbation corrections (full line). Not only the minimum is reached at different values of η , but also the absolute value as well as the curvature at the minimum are different.

TABLE III. Results for the optical response of Na_8 . The energy position of the surface-plasmon peak in electron volts is given for the different geometries and different minima displayed in Table I, obtained making use of the HA-PSP. For comparison, the jellium results both at the LDA level and the FULL-SIC level, taken from Ref. 14 are shown. Under the column Expt., the experimental value taken from Ref. 21 is tabulated.

Na_8	Jellium		D_{2d}		D_{4d}		T_d		Expt.
	LDA	FULL-SIC	$E_{\text{HA}}^{(0)}$	$E_{\text{HA}}^{(2)}$	$E_{\text{HA}}^{(0)}$	$E_{\text{HA}}^{(2)}$	$E_{\text{HA}}^{(0)}$	$E_{\text{HA}}^{(2)}$	
E_{peak}	2.73	2.50	2.49	2.56	2.51	2.58	2.40	2.48	2.52

The dashed curve corresponds to $E_{\text{HA}}^{(0)}$ whereas the full curve corresponds to $E_{\text{HA}}^{(2)}$. In addition to the different bond lengths, a remarkable lowering of the total energy takes place as a consequence of second-order pseudopotential perturbation theory. Furthermore, we expect to find important modifications in, e.g., abundance spectra, due to changes in the highest occupied molecular orbital–lowest unoccupied molecular orbital (HOMO-LUMO) gaps, which will make some “magic” numbers less “magic.” Changes in the HOMO-LUMO gap will also imply important modifications in dynamical properties of these systems as well as in their relative stability as a function of internal temperature.

B. Optical absorption

1. Closed-shell systems

In the next step we calculate, with the monopole part of the external potential, the optical response of Na_8 and Na_{20} . We restricted ourselves to the HA-PSP due to its better performance than the A-PSP. All response calculations were carried out for values of the scaling parameters which minimize both total-energy expressions discussed before, for each geometry and pseudopotential. The dynamical response of Na_8 is very similar for all the line shapes computed. The main feature of all these response calculations is a single prominent peak which exhausts most of the Thomas-Reiche-Kuhn sum rule, and which is associated with the excitation of the surface plasmon in this small cluster. For Na_{20} , all the line shapes computed are dominated by two main peaks, which also exhaust most of the sum rule. However, and for both clusters, small fractions of this sum rule are redistributed in a different way for each calculation, a feature related to the resulting one-electron level distribution in the monopole external potential. Furthermore, the energy location of the one (two) peak(s) in Na_8 (Na_{20}) changes significantly as a function of pseudopotential and total-energy minimization criteria. This points to the main effect of the pseudopotentials, which is to fix the volume of delocalization of the valence electrons. This feature is illustrated in Tables III (for Na_8) and IV (for Na_{20}), where we show the energy associated with the one (two) peak(s) for Na_8 (Na_{20}) for the different geometries and, for each geometry, at the two configurations resulting from total-energy minimization using ($E^{(0)}$) and ($E^{(2)}$). Also given in Tables IV and V are the experimental results from Ref. 21, together with the results from

the standard jellium model in LDA, as well as the results using the jellium model in self-interaction corrections (FULL-SIC).¹⁴

For the internal temperatures at which the experiments have been carried out, it is unlikely that Na_8 (and also Na_{20}) will be trapped in an isomeric state. Therefore, the closest static configuration we can use is the one corresponding to the ground state.²² In this spirit, the most likely result among the tabulated values gives 2.56 eV for Na_8 and 2.51 and 2.77 eV for the two peaks of Na_{20} . This represents a big improvement with respect to the standard jellium model, while the peak position remains blue-shifted with respect to the experimental data. This is gratifying, since from previous studies,¹⁴ we know that SIC lead to sizeable effects in the optical response, especially for small clusters (cf., e.g., Tables IV and V). These SIC, among other features, systematically induce a redshift of the peak position, which nicely correlates with the present results.²⁴

As already pointed out, important shifts take place due to the inclusion of the ionic structure. However, all these shifts can be understood as a volume effect. Indeed, the global energy minimization with inclusion of the ionic structure leads to another volume of delocalization for the loosely bound electrons, that is, the ions act to change the value of n_0 in Eq. (1). In spite of this change, the effect of the ions is rather primitive, at least for the small clusters studied in this work: band-structure effects, which would manifest themselves in “bulk quantization” instead of surface quantization (that is, quantum-size effects), or in additional gaps instead of those introduced by the surface, though present, are small. In Fig. 5 we show the line shapes associated with the photoabsorption

TABLE IV. Results for the optical response of Na_{20} . The energy position (electron volts) of the two dominating peaks associated with the excitation of the surface-plasmon resonance are given for the different geometries and different minima displayed in Table I, obtained making use of the HA-PSP. For comparison, the jellium results both at the LDA level and the FULL-SIC level, taken from Ref. 14 are shown. Under the column Expt., the experimental results of Ref. 21 are tabulated.

Na_{20}	Jellium		A		B		Expt.
	LDA	FULL-SIC	$E_{\text{HA}}^{(0)}$	$E_{\text{HA}}^{(2)}$	$E_{\text{HA}}^{(0)}$	$E_{\text{HA}}^{(2)}$	
$E_{\text{peak 1}}$	2.67	2.48	2.42	2.51	2.43	2.56	2.46
$E_{\text{peak 2}}$	2.96	2.78	2.68	2.77	2.69	2.82	2.74

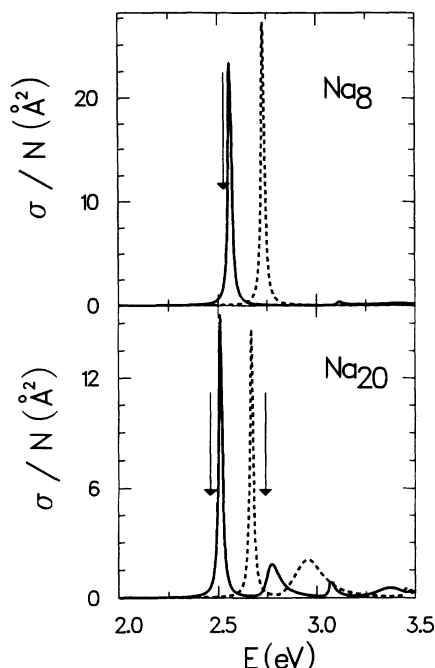


FIG. 5. Line shapes of the photoabsorption cross section per valence electron for Na_8 and Na_{20} , calculated with TDLDA. Two curves are shown for each cluster: The solid line corresponds to the result of the present formulation (see main text for details), the dashed line corresponds to the result of the standard jellium model. The experimental features are illustrated with arrows, which show the position of the main peaks which have been resolved experimentally.

cross section of Na_8 and Na_{20} . The dotted lines show the results obtained with the structureless jellium model,¹⁴ whereas the full lines show the results of the present calculations, carried out for the D_{2d} structure of Na_8 and the A structure of Na_{20} at the minima obtained using the Ha-PSP pseudopotential perturbation corrections. The vertical arrows show the energy position of the main peak(s) identified experimentally (cf. Tables III and IV). While the main effect for Na_8 is an overall shift of the plasmon peak, for Na_{20} one can observe some additional effects. Besides the redistribution of strength, additional structure develops in the UV part of the spectrum which was previously absent in the jellium results. Experiments up to date have not explored this part of the spectrum. Furthermore, it remains an open question whether this UV structure, which was also found in jellium-FULL-SIC calculations¹⁴ will be enhanced or reduced when both ionic structure effects and SIC are included simultaneously.

2. Effects of the non-SAPS part of the external pseudopotential

First, we study the effect of $v_{2,\text{ext}}$, Eq. (3), on the optical absorption of a *magic* cluster, namely, Na_8 in its ground-state configuration D_{2d} . Figure 6 shows as the dashed line the result, which peaks at the value of 2.6 eV, the continuous line gives as comparison the SAPS-

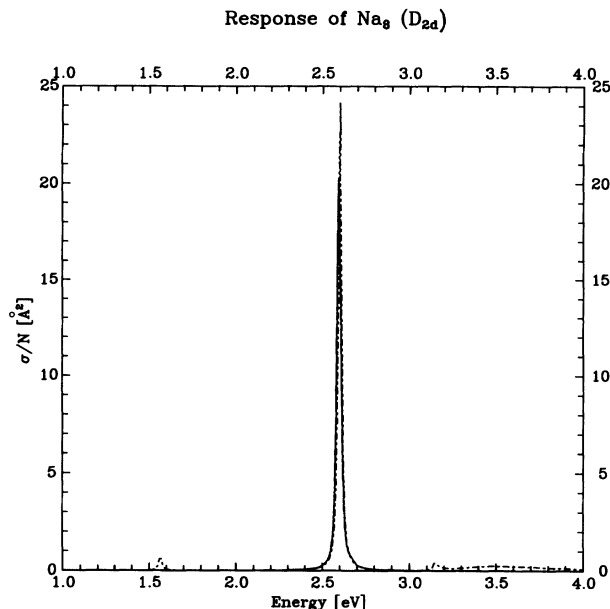


FIG. 6. Photoabsorption cross section $\sigma(\omega)$ per delocalized electron for Na_8 in its ground-state geometry, D_{2d} , at two levels of calculation: dashed line, SAPS model; continuous line, effects of full symmetry [$v_{2,\text{ext}}$, Eq. (3)]. For further explanations see main text.

TDLDA results, which is nearby.²⁵ By the close proximity of the two curves, we obtain at least *a posteriori* a justification of the SAPS model for *magic* number clusters. This is the first and important result of the present study (which was to be expected, of course).

In the next step, we study the effect of $v_{2,\text{ext}}$ on the optical absorption of open shell clusters, with Na_6 and Na_{10} as examples. The geometries, shown in Fig. 7, are again taken from Ref. 13, and here we adopt the ground-state configurations, which are C_{5v} and the a structure of (Ref. 13) for Na_6 and Na_{10} , respectively.

Figure 8 shows the cross section per delocalized electron of Na_6 at two different levels. The dashed line gives the SAPS result, which is too crude to reproduce the experimental result. On contrast the full calculation (con-

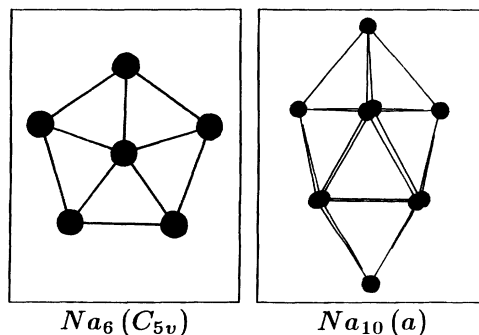


FIG. 7. Geometries used for the two open-shell clusters Na_6 and Na_{10} . Both symmetry and bond length are taken from Ref. 13.

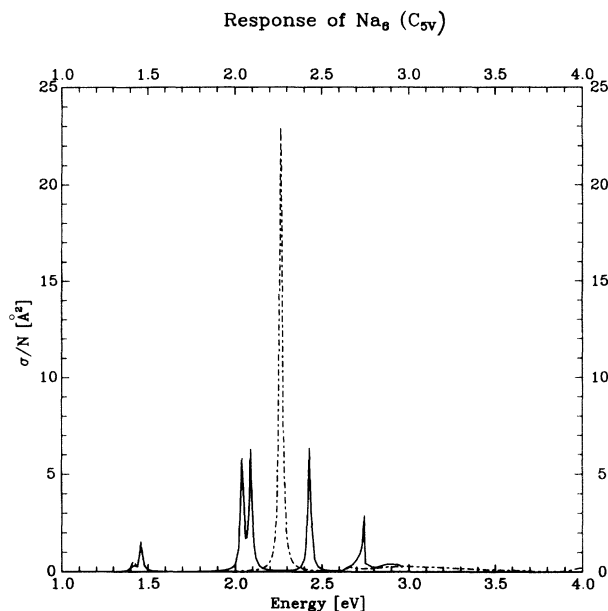


FIG. 8. Photoabsorption cross section $\sigma(\omega)$ per delocalized electron for Na_6 in its ground-state configuration (see Fig. 7). Dashed line, SAPS model used for the effects of the ionic structure, which is clearly insufficient; continuous line, full symmetry taken into account. The continuous curve agrees quantitatively with the experimental data of (Ref. 26).

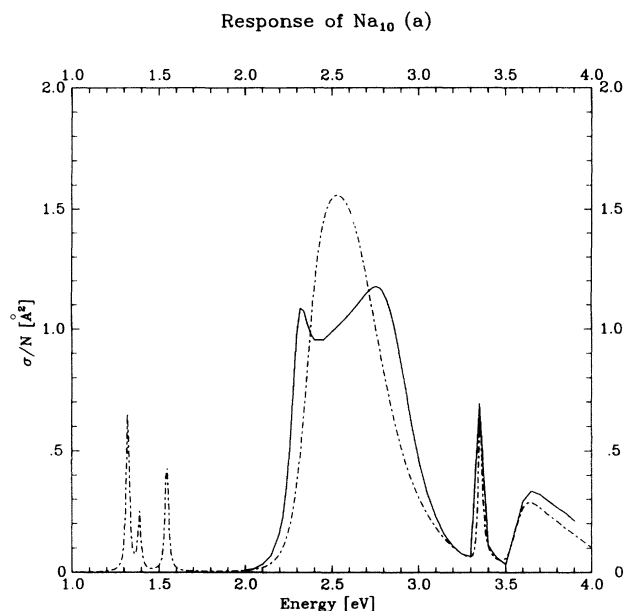


FIG. 9. Photoabsorption cross section $\sigma(\omega)$ per delocalized electron for Na_{10} in its ground-state configuration (see Fig. 7). Dashed line, SAPS model; continuous line, full symmetry taken into account. Surprisingly enough, the full spectrum does *not* resemble that of the spheroidal jellium model.⁶

tinuous line) is in qualitative agreement not only with the experimental results by Wang *et al.*²⁶ but also with the results of Bonačić Koutecký *et al.*¹⁸ The small splitting around 2 eV is not resolved experimentally, but the remaining features agree qualitatively with Ref. 26. Surprisingly enough, the spectrum of Na_{10} (see Fig. 9) does *not* resemble that of the spheroidal jellium model by Ekardt and Penzar,⁶ which seems to indicate a pronounced effect beyond the jellium approximation, whereas the results for the magic clusters fully corroborate the jellium approximation.

IV. CONCLUSIONS

Second-order pseudopotential perturbation theory seems to provide a simple and efficient method to study ionic effects in jellium alkali clusters. The good agreement we obtained with fully-relaxed total-energy minimizations corroborates this picture.

Finally, we would like to add some general remarks related to the TDLDA. While there is *no* theorem which states the existence of a time-dependent density-functional like the Hohenberg-Kohn theorem for the ground state, there is a perturbational consideration by Gross and Kohn²⁷ which shows to which extent the TDLDA can be justified. But above all doubts of princi-

ple, it has been shown by Zangwill and Soven,²⁸ by Levine and Soven,²⁹ and by Quong and Eguiluz that TDLDA “works” marvelously well in the case of atoms, molecules, and solids, respectively. Therefore we conclude that, if the best wave functions are used, one should be able to achieve a quantitative description in the case of clusters as well (indeed, the results on Na_6 are competitive with Ref. 18).

At present it remains to be demonstrated, whether or not this type of study can really be extended to very large clusters in order to approach the semi-infinite half space; in principle, it should be possible because we know from Landman’s work¹¹ that surface layer relaxation can be predicted successfully within second-order pseudopotential perturbation theory. Furthermore, we know from the work of Quong and Eguiluz³⁰ that the wave functions obtained with our procedure can be used as input in a forthcoming TDLDA calculation of plasmons in quantitative agreement with experiment.

ACKNOWLEDGMENTS

We are grateful to Professor E. Zeitler for continuous interest and support. J.M.P. thanks the Max-Planck-Gesellschaft for financial support. This project is supported by the DAAD within its INIDA project.

¹G. D. Mahan, *Many-Particle Physics* (Plenum, New York, 1981).

²W. Ekardt and Ber. Bunsenges, *Phys. Chem.* **88**, 289 (1984); *Phys. Rev. Lett.* **52**, 1925 (1984); *Phys. Rev. B* **29**, 1558 (1984).

³M. Brack, *Rev. Mod. Phys.* **65**, 677 (1993).

⁴A. G. Eguiluz, *Phys. Rev. B* **35**, 5473 (1987).

⁵W. Ekardt, *Phys. Rev. B* **32**, 1961 (1985).

⁶W. Ekardt and Z. Penzar, *Phys. Rev. B* **43**, 1322 (1991); **38**,

- 4273 (1988); Z. Penzar, and W. Ekardt, *Z. Phys. D* **17**, 69 (1990).
- ⁷J. G. Eaton *et al.*, in *Nuclear Physics Concepts in the Study of Atomic and Cluster Physics*, edited by R. Schmidt, H. O. Lutz, and R. Dreizler, Lecture Notes in Physics Vol. 404 (Springer, New York, 1992).
- ⁸L. Serra, G. B. Bachelet, N. Van Giai, and E. Lipparini, *Phys. Rev. B* **48**, 14 708 (1993).
- ⁹C. A. Utreras-Diaz and H. B. Shore, *Phys. Rev. B* **40**, 10 345 (1989).
- ¹⁰J. P. Perdew, H. Q. Tran, and E. D. Smith, *Phys. Rev. B* **42**, 11 627 (1990).
- ¹¹R. N. Barnett, Uzi Landman, and C. L. Cleveland, *Phys. Rev. B* **27**, 6534 (1983).
- ¹²M. P. Iñiguez, M. J. Lopez, J. A. Alonso, and J. M. Soler, *Z. Phys. D* **11**, 163 (1989).
- ¹³U. Röthlisberger and W. Andreoni, *J. Chem. Phys.* **94**, 8129 (1991).
- ¹⁴J. M. Pacheco and W. Ekardt, *Ann. Phys. (Leipzig)* **B 1**, 254 (1992).
- ¹⁵B. H. Bransden and C. J. Joachain, *Physics of Atoms and Molecules* (Longman, London, 1983).
- ¹⁶We would like to point out, however, that only for some simple metals of groups Ia and Ib one may expect this to happen. For clusters of other systems, local pseudopotentials may not describe adequately the electron-ion interaction.
- ¹⁷J. L. Martins, J. Buttet, and R. Car, *Phys. Rev. B* **31**, 1804 (1985).
- ¹⁸V. B. Koutecký *et al.*, *Chem. Rev.* **91**, 1035 (1991), and references therein.
- ¹⁹The different bond lengths found in the framework of Ref. 18 might be one of the reasons why the single-particle levels are markedly different from the jellium results, whereas those found in Ref. 13 agree not only qualitatively but also quantitatively (for sodium) with the jellium results.⁶
- ²⁰For the sodium dimer, the norm-conserving pseudopotential used in Ref. 13 leads to errors in the bond-length and vibrational frequency which do not exceed 2% (compare, e.g., Ref. 18).
- ²¹K. Selby *et al.*, *Phys. Rev. B* **43**, 4565 (1991).
- ²²In carrying out a dynamical response for a single static configuration of our system, we are neglecting important effects associated with quantal and thermal fluctuations of the clusters.²³ However, at the level considered here, we find that the line shapes are rather insensitive to the underlying symmetry of the cluster. This means, in turn, that the net effect of including fluctuations (at least in the spirit of the Born-Oppenheimer approximation inherent to the present work) would be mainly to enlarge the different peaks, without significantly changing their position. The tabulated values correspond simply to the peak positions for the most probable configuration of the systems.
- ²³J. M. Pacheco and R. A. Broglia, *Phys. Rev. Lett.* **62**, 1400 (1989); G. F. Bertsch and D. Tománek, *Phys. Rev. B* **40**, 2749 (1989); C. Yannouleas, J. M. Pacheco, and R. A. Broglia, *et al.*, *ibid.* **41**, 6088 (1990); Z. Penzar, W. Ekardt, and A. Rubio, *ibid.* **42**, 5040 (1990); J. M. Pacheco, R. A. Broglia, and B. R. Mottelson, *Z. Phys. D* **21**, 289 (1991).
- ²⁴We would like to point out that we feel it is not correct to apply the SIC directly to the present formulation. Therefore we did not perform any SIC here, deferring this problem to a forthcoming publication.
- ²⁵The reason that it does not peak at 2.56 eV (see Table III) is caused by the fact that the coordinates used are exactly those of Ref. 13, whereas in Table III we used scaled coordinates (see Table I).
- ²⁶C. R. Wang, St. Pollack, T. A. Dahlseid, and G. M. Koretsky, *J. Chem. Phys.* **96**, 7931 (1992).
- ²⁷E. K. U. Gross and W. Kohn, *Adv. Quantum Chem.* **21**, 255 (1991).
- ²⁸A. Zangwill and P. Soven, *Phys. Rev. B* **21**, 1561 (1980).
- ²⁹Z. Levine and P. Soven, *Phys. Rev. A* **25**, 625 (1984).
- ³⁰A. A. Quong and A. G. Eguiluz, *Phys. Rev. Lett.* **70**, 3955 (1993).